

Abstract

Asymmetries in plasma density irregularity generation between the leading and trailing edges of large-scale plasma density structures in the high-latitude ionosphere are investigated. A model is developed that evaluates the gradient-drift instability (GDI) growth rate differences across the gradient reversal that is applicable at all propagation directions and for a broad range of altitudes spanning the entire lower ionosphere. In particular, the model describes asymmetries that would be observed by an oblique scanning radar near density structures in the polar cap such as polar patches. The dependencies on the relative orientations between the directions of the gradient reversal, plasma convection, and wave propagation are examined at different altitudinal regions. At all altitudes, the largest asymmetries are expected for observations along the gradient reversals, e.g. when an elongated structure is oriented along the radar boresite. The convection direction that results in the strongest asymmetries exhibits a strong dependence on the altitude, with the optimal convection being parallel to the gradient reversal in the E region, perpendicular to it in the F region, and at some angle between these extremes in the transitional region.

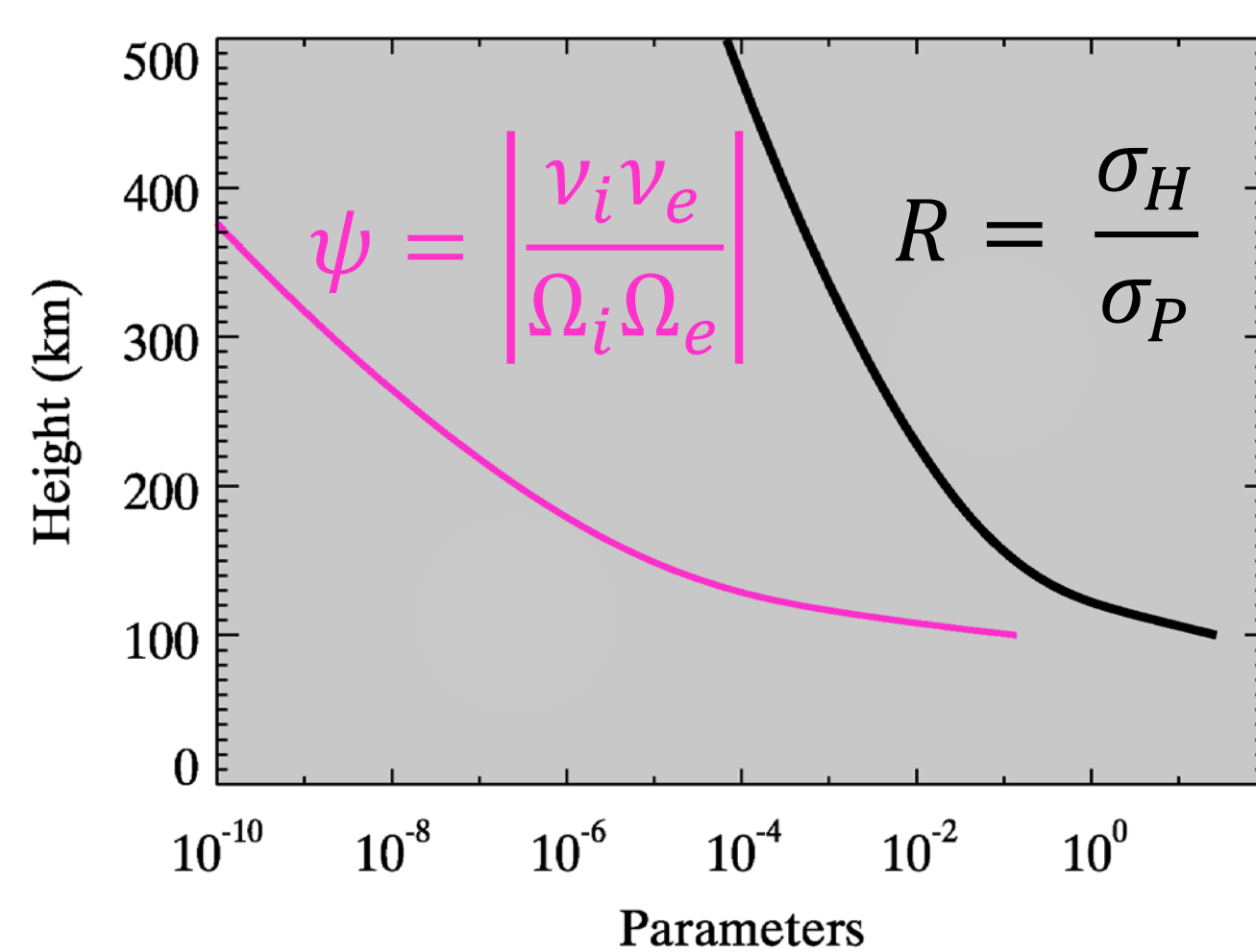
Introduction

The gradient-drift instability (GDI) allows for wave growth when a drifting plasma has a density gradient. Observations have found asymmetries between the leading and trailing edges of large-scale density structures in the ionosphere (e.g. Weber et al., 1984; Milan et al., 2002). GDI linear theory can be applied to the field of view (FoV) of a HF coherent scatter radar, such as in the Super Dual Auroral Radar Network (SuperDARN), to provide some insight into this phenomenon.

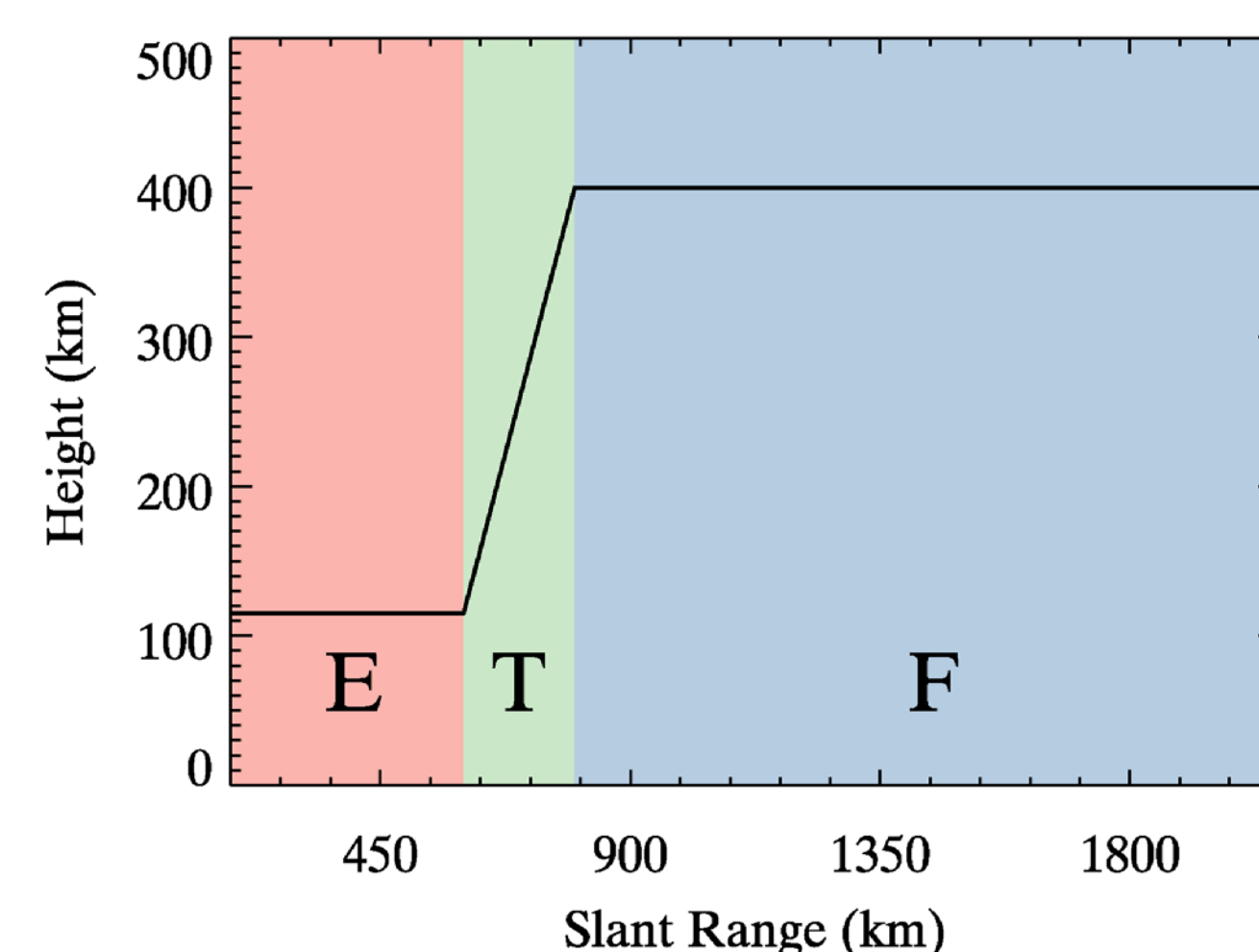
Linear GDI growth rate (Makarevich, 2014):

$$\gamma = \frac{GV_E}{1 + \psi} (\hat{k} \cdot \hat{b} \times \hat{g})(\hat{k} \cdot \hat{e} - R\hat{k} \cdot \hat{e} \times \hat{b})$$

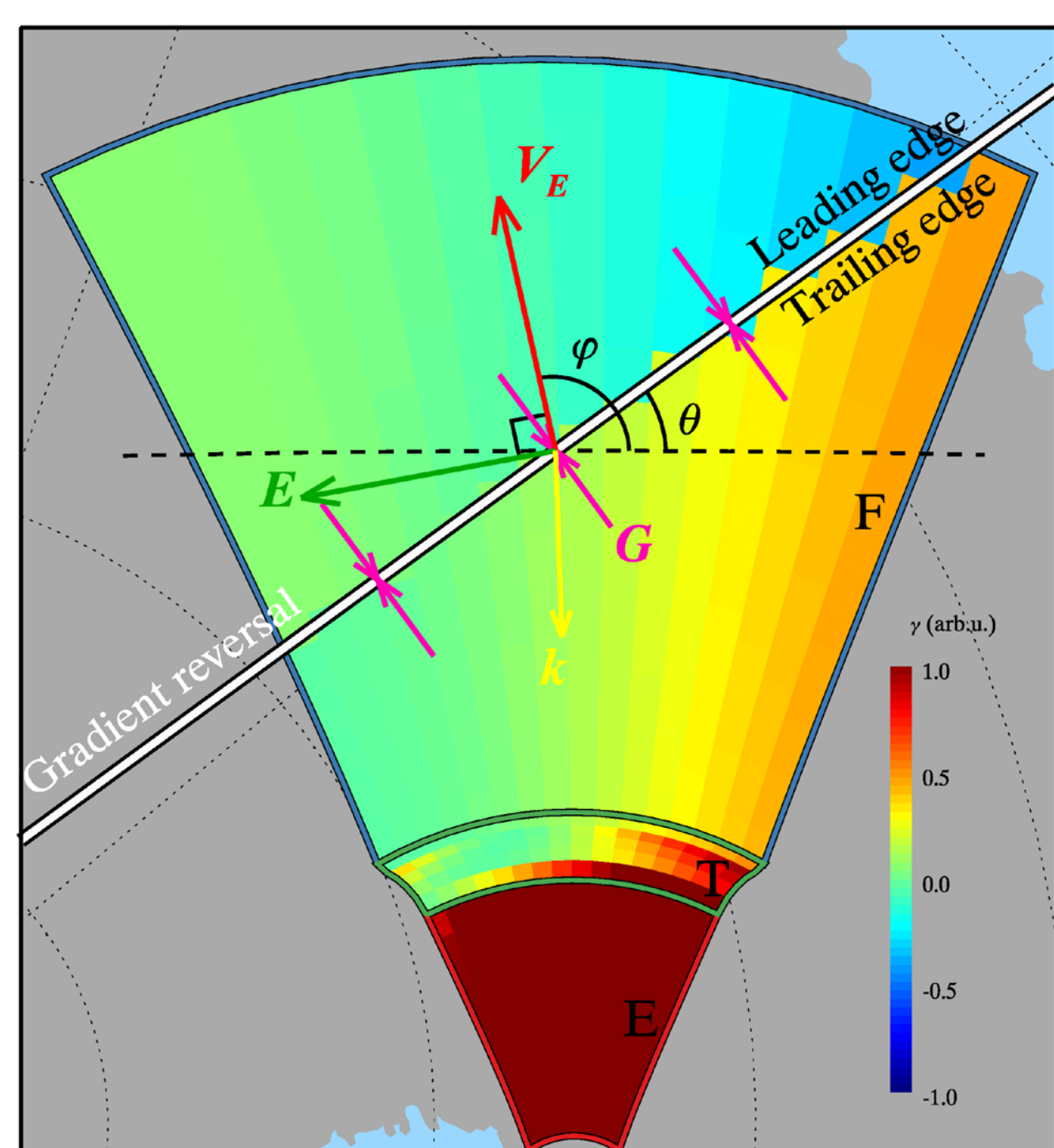
Dependent on:
Direction - \hat{k}
Altitude - R



Height dependence of the anisotropy parameter, ψ , and the conductivity ratio, R . Both decrease by several orders of magnitude between E-region and F-region altitudes.

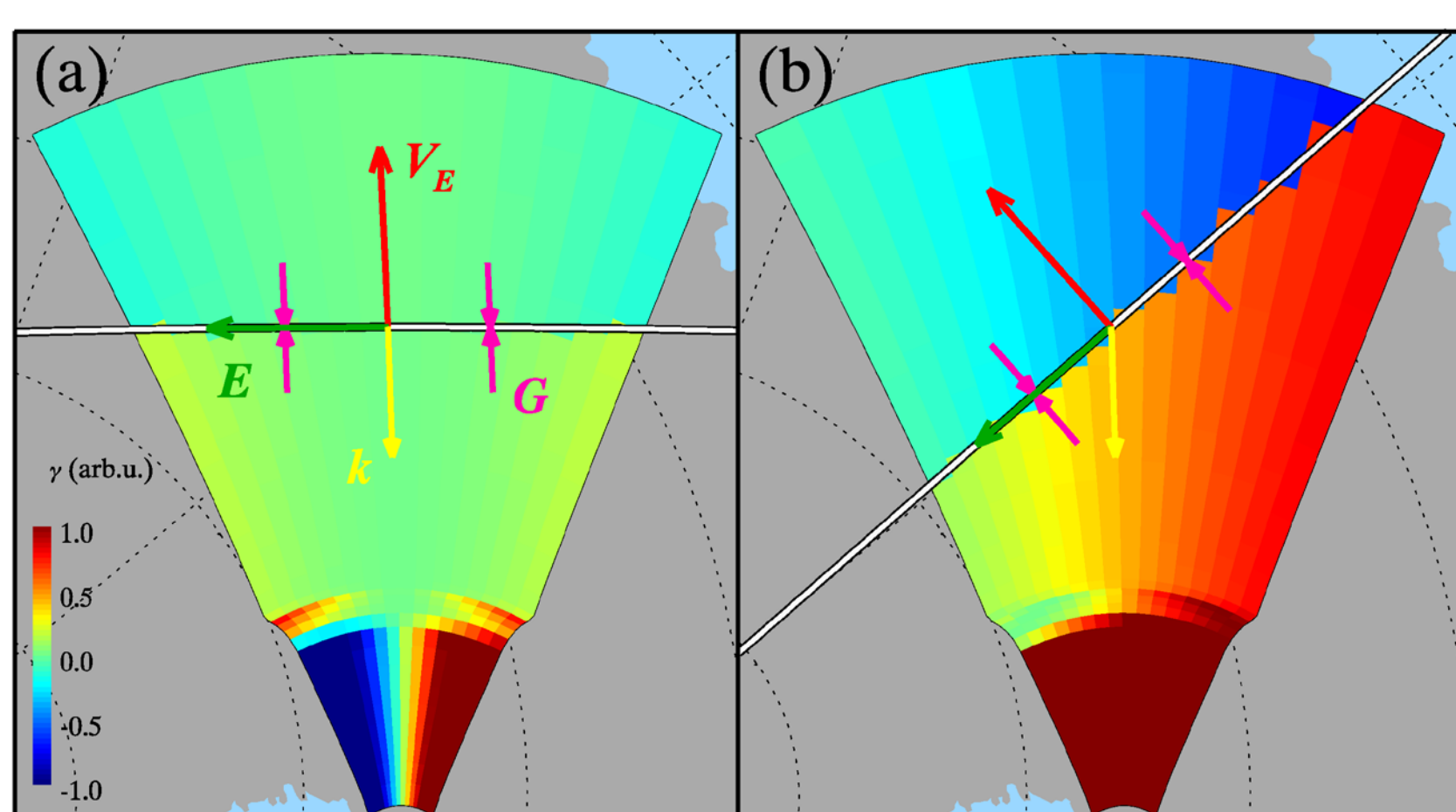


Height of SuperDARN HF radar beam. Different slant ranges sample the E region, F region, and a transitional region between the two.



- Black-white line represents large-scale density gradient reversal
- Uniform field of gradient magnitudes
- Gradient direction reverses at the line
- Gradient reversal direction: θ
- Convection direction: ϕ
- Vary both θ and ϕ independently
- Large $\gamma \rightarrow$ greater structuring \rightarrow more observed backscatter

GDI growth rate at each cell within the McMurdo Station SuperDARN FoV for a particular gradient reversal and convection direction.

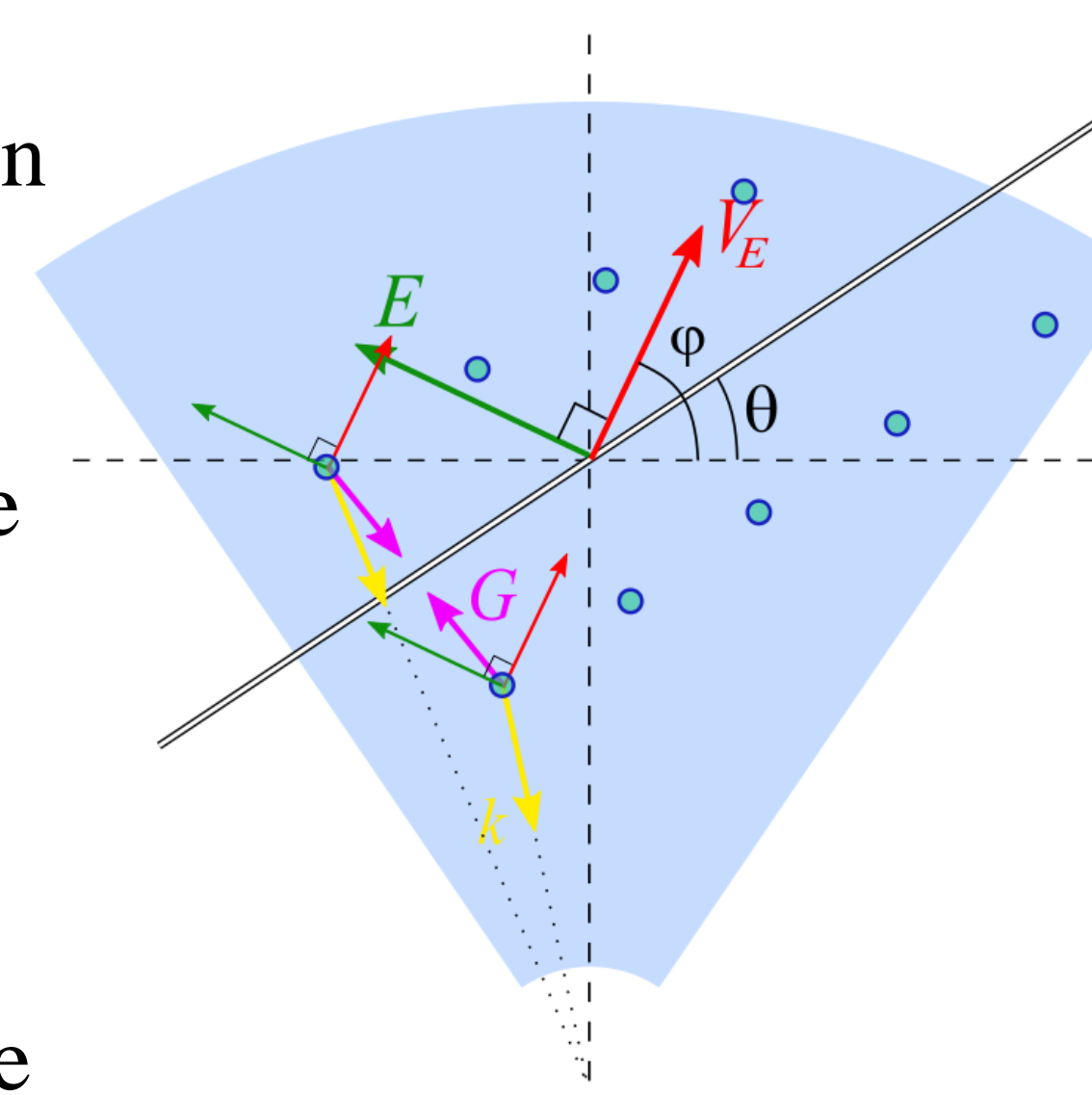


- Different orientations produce different degrees of contrast in the growth rate
- Asymmetry in growth rate implies asymmetry in observed backscatter
- Need to quantify contrast over entire FoV

Methods for Quantifying Asymmetry

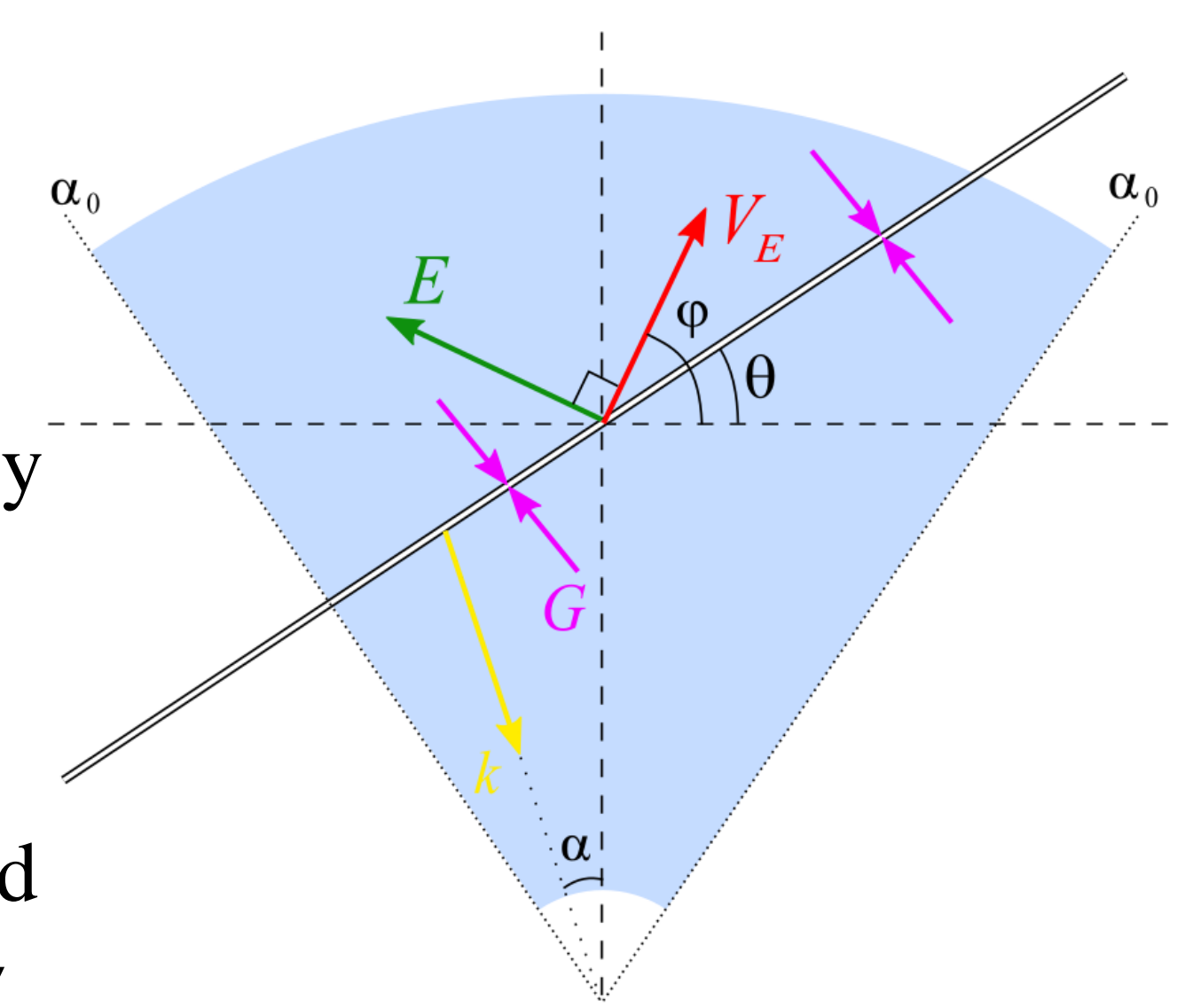
Numerical

1. Consider a series of points within the FoV that are mirrored over the gradient reversal
2. Find wavevector (\vec{k}) and altitude (R) for virtual beam
3. Find the growth rate at each point
4. Subtract trailing edge point γ from corresponding leading edge point γ for $\Delta\gamma$
5. Average over all point pairs



Analytic

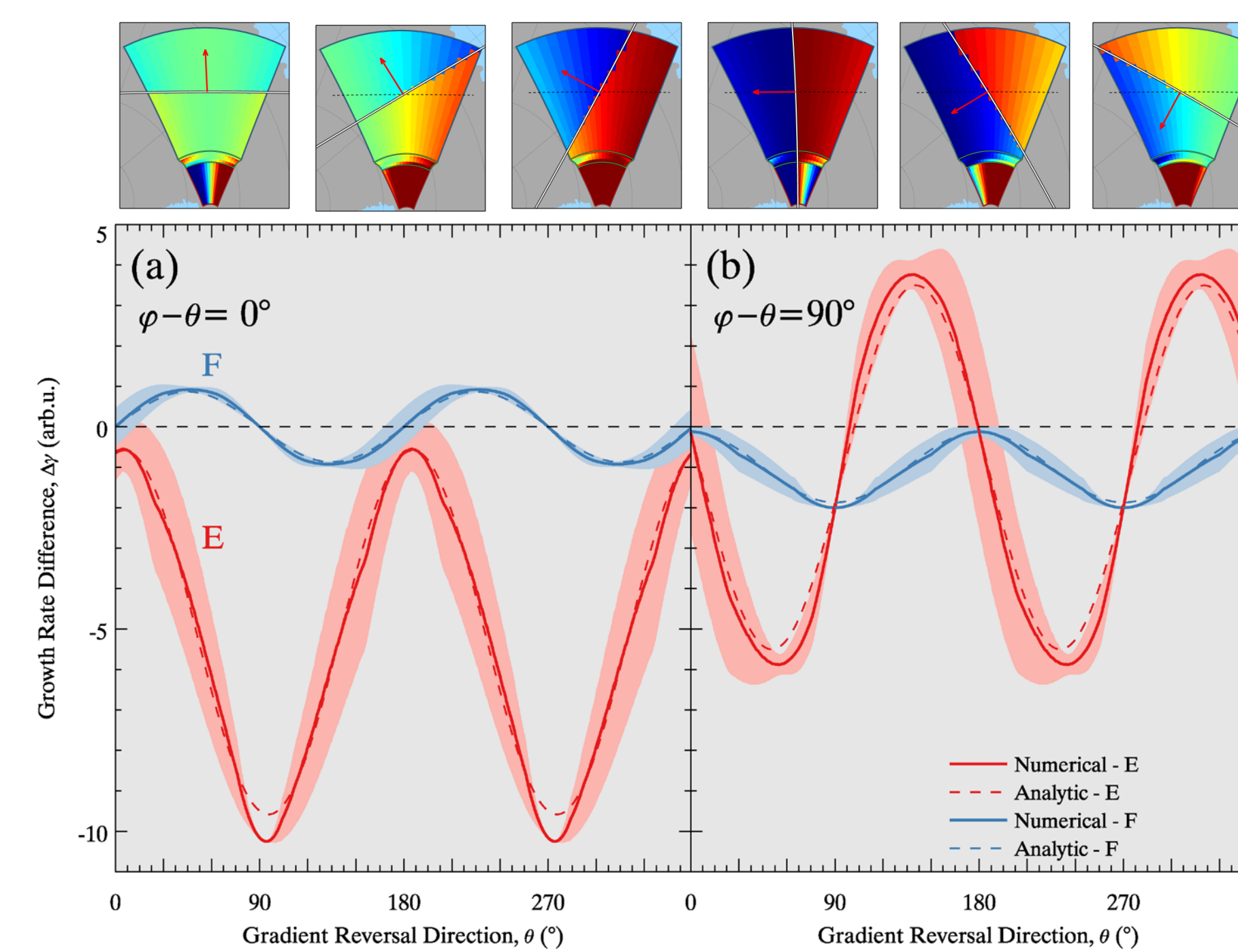
1. Consider a point on the gradient reversal within FoV
2. Wavevector, \vec{k} , defined by angle with boresight, α
3. Find $\Delta\gamma$ in terms of α , θ , and ϕ
4. Integrate over FoV to find expression for average $\Delta\gamma$



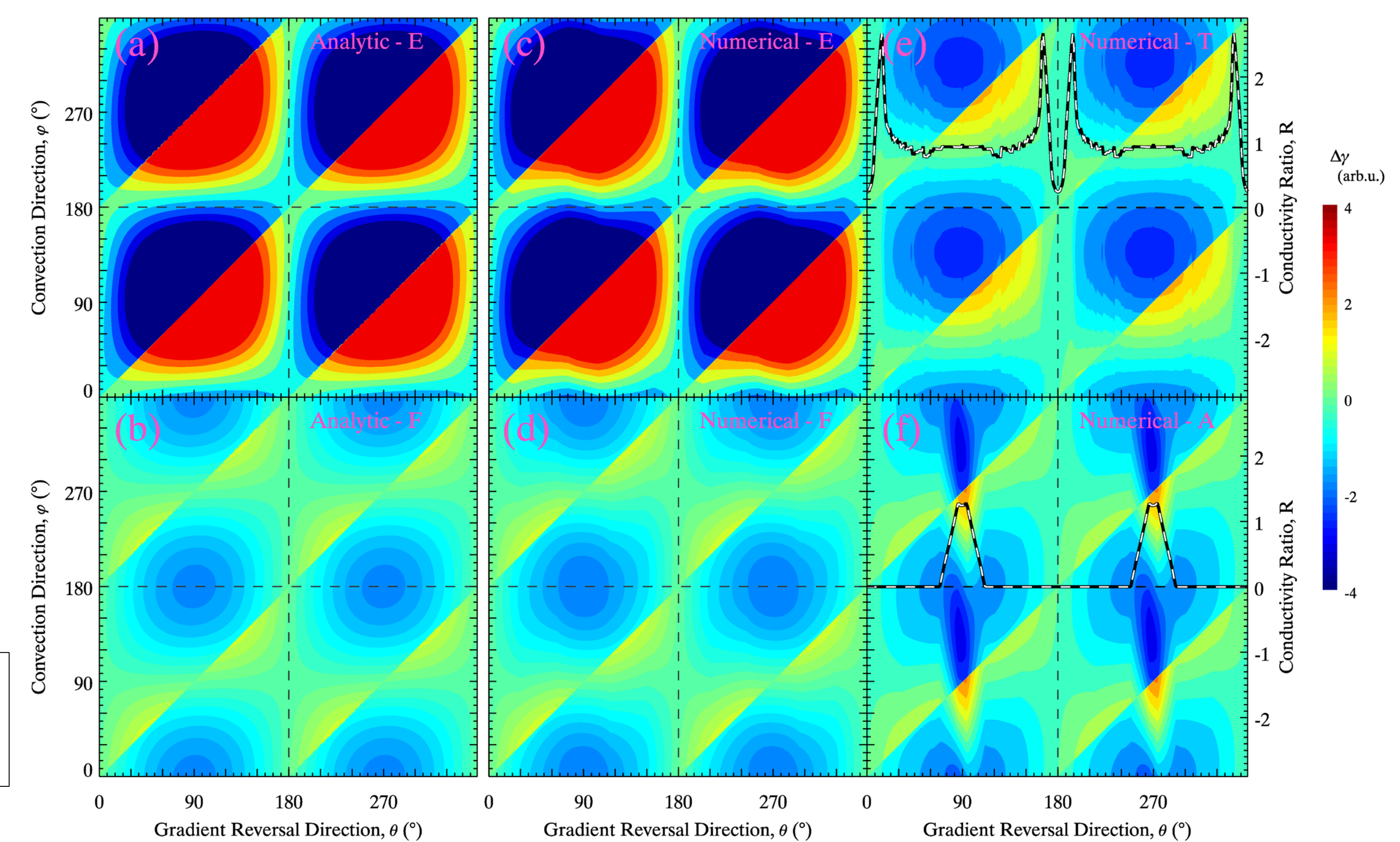
$$\Delta\gamma = H(\theta, \phi) [\sin(\phi - \theta) - C \sin(\phi + \theta) + R(\cos(\phi - \theta) - C \cos(\phi + \theta))]$$

$$H(\theta, \phi) = \Theta(\phi - \theta + \pi) - \Theta(\theta - \phi - \pi) + 2\Theta(\phi - \theta - \pi) - 2\Theta(\phi - \theta)$$

Results

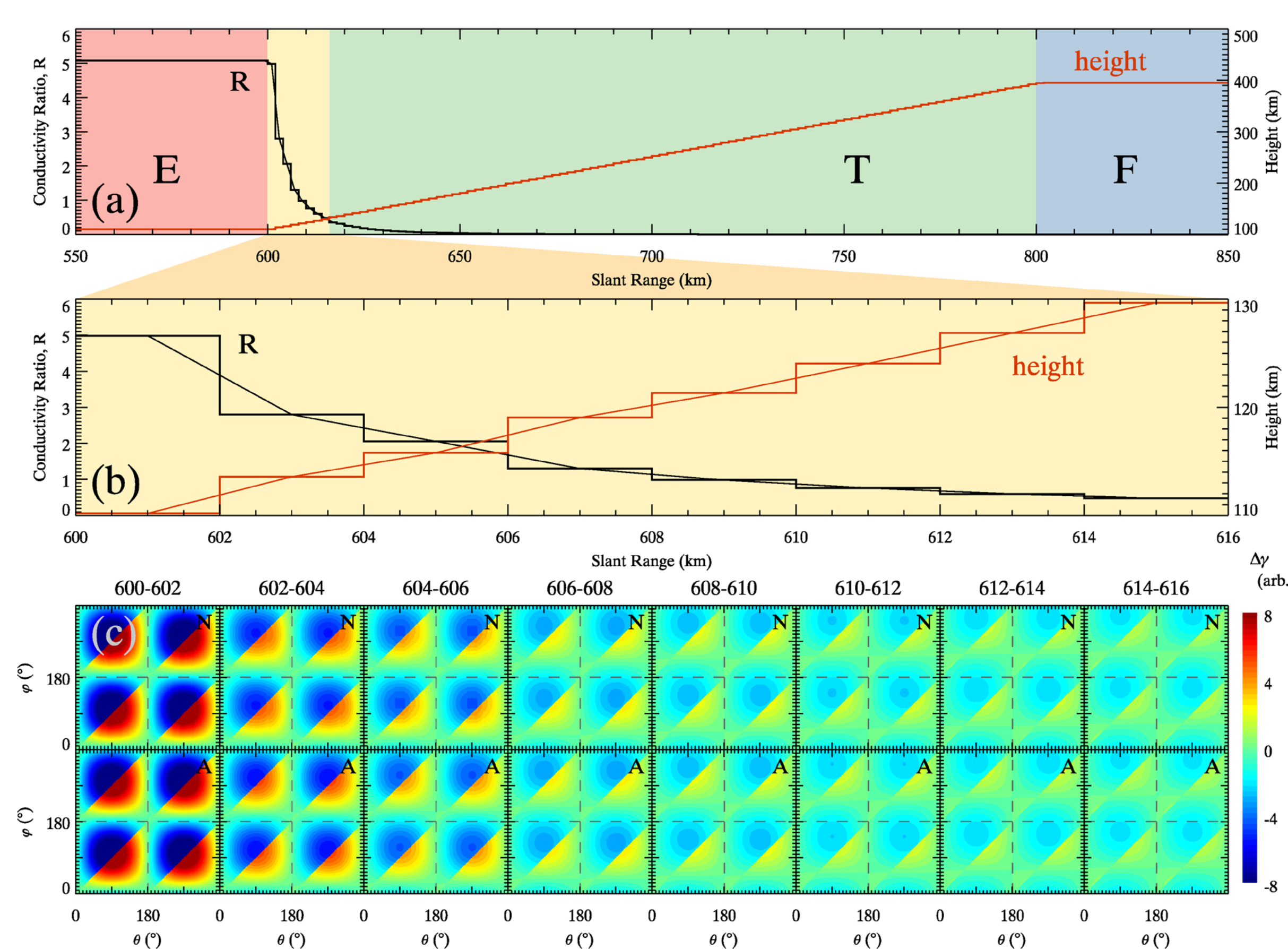


Average $\Delta\gamma$ across the gradient reversal with the convection direction, ϕ , being either (a) parallel to or (b) perpendicular to the gradient reversal direction, θ .



E region maximum $\Delta\gamma$: $\theta = 90^\circ, 270^\circ$; $\phi = 90^\circ, 270^\circ$
F region maximum $\Delta\gamma$: $\theta = 90^\circ, 270^\circ$; $\phi = 0^\circ, 180^\circ$

Average $\Delta\gamma$ across the gradient reversal for any arbitrary gradient reversal direction, θ , and convection direction, ϕ . Analytic: panels a-b; numerical: panels c-f. E region: panels a & c; F region: panels b & d; transitional region: panel e; all regions: panel f.



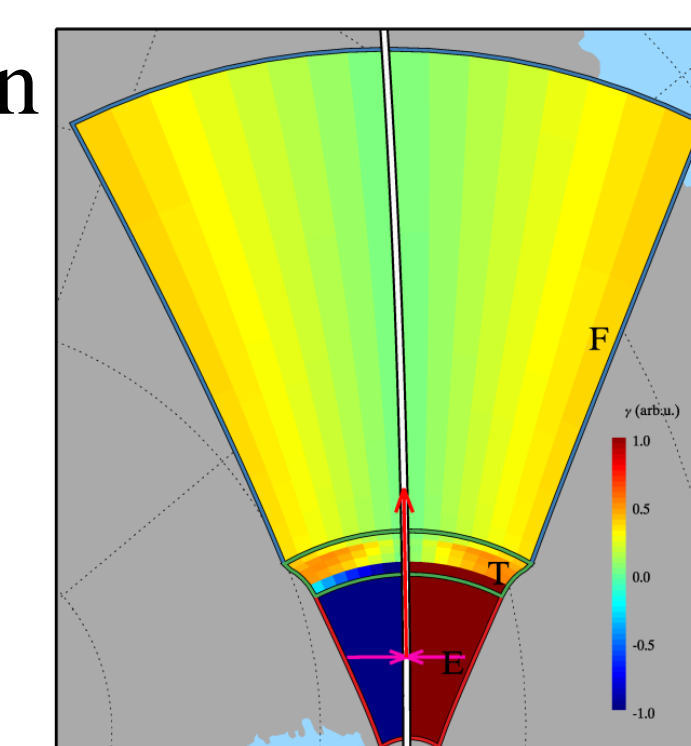
Analysis of the transitional region between E and F region altitudes.

- R decreases by several orders of magnitude
- $\Delta\gamma$ smoothly transitions from E region to F region pattern
- Low sensitivity to changes in altitude above 130 km

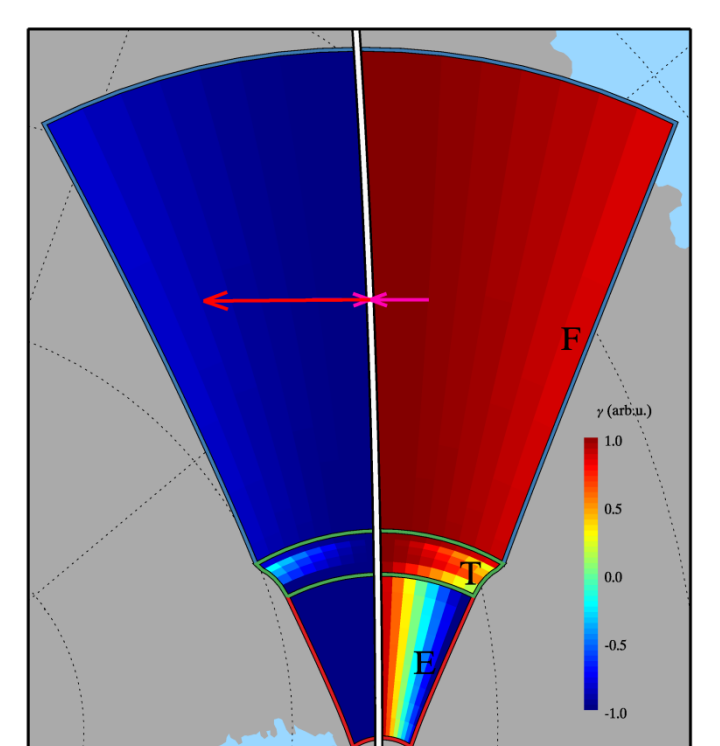
Conclusions

1. Asymmetry is maximized when \vec{k} is parallel to the gradient reversal

E Region
 $\vec{V}_E \perp \vec{G}$



F Region
 $\vec{V}_E \parallel \vec{G}$



2. Asymmetry magnitude is almost always negative in the F region, implying more structuring on the trailing edge
3. Large scale density structures in the F region are most likely to be observed by an oblique scanning radar when they are parallel to the radar boresite

Acknowledgements

This work was supported by NSF grants AGS-1248127 and PLR-1443504. The MSISE-90 model is available from the GSFC/SPDF OMNIWeb interface at <http://omniweb.gsfc.nasa.gov/>.

References

- Makarevich, R. A.: Symmetry considerations in the two-fluid theory of the gradient-drift instability in the lower ionosphere, *J. Geophys. Res.*, 119, doi:10.1002/2014JA020292, 2014.
- Milan, S. E., Lester, M., Yeoman, T. K.: HF radar polar patch formation revisited: summer and winter variations in dayside plasma structuring, *Ann. Geophysicae*, 20, 487-499, 2002.
- Weber, E. J., Buchau, J., Moore, J. G., Sharber, J. R., Livingston, R. C., Winningham, J. D., and Reinisch, B. W.: F layer ionization patches in the polar cap, *J. Geophys. Res.*, 89, 1683-1694, 1984.